ISSN 0036-0244, Russian Journal of Physical Chemistry A, 2019, Vol. 93, No. 6, pp. 1065–1072. © Pleiades Publishing, Ltd., 2019.

PHYSICAL CHEMISTRY OF SOLUTIONS

Molecular Interactions in Solutions of 1,1-Bis(4-(2-oxopropoxy)phenyl)cyclohexane on Ultrasonic Velocity, Density, and Viscosimetric Data[1]

Bh. B. Dhaduk[a,b] and P. H. Parsania[b,*]

[a] *Department of Chemistry, School of Science, RK University, Gujarat, Rajkot-360004 India*

[b] *Polymer Division, Department of Chemistry, Saurashtra University, Gujarat, Rajkot-360005 India*

**e-mail: phparsania@aol.com, phparsania22@gmail.com*

Received May 19, 2018; revised July 13, 2018; accepted December 20, 2018

Abstract—The ultrasonic velocity, density, and viscosity are measured at various concentrations 0.1–0.01 mol dm^{-3} in the solutions of 1,1-bis(4-(2-oxopropoxy)phenyl)cyclohexane (BMAPC) in 1,4-dioxane (DO), ethyl acetate (EA), tetrahydrofuan (THF) at 298–313 K and at atmospheric pressure. Parameters: acoustical impedance, adiabatic compressibility, Rao's molar sound function, Van der Waals constant, internal pressure, free volume, intermolecular free path length, classical absorption coefficient and viscous relaxation time, Gibbs free energy of activation, enthalpy of activation and entropy of activation were determined. Change of the parameters with *T* indicated existence of strong molecular interactions in solutions and further supported by positive values of solvation number. Gibbs free energy of activation decrease linearly with increasing *C* and *T* in the DO system while it decreases with *C* and increase with *T* in EA and THF. Enthalpy and entropy of activation were found to be slightly concentration dependent.

Keywords: ultrasonic speed, acoustical parameters, thermodynamic parameters

DOI: 10.1134/S0036024419060086

INTRODUCTION

Bisphenols are very important compounds for the synthesis of thermally stable polymers, resins and plastic materials [1–3]. In recent years, bisphenols and their derivatives were found to be effective fungicides and plant growth regulators [4–6]. So, the process of transportation and biological effect of such molecules across the biological membrane is very important to understand and that has been carried out by measuring ultrasound velocity [7, 8]. Measurement of ultrasonic velocity provides information about molecular size, shape and strength of molecular interactions of pure liquids, liquid mixtures and organic compounds [9–11].

1,1-Bis(4-(2-oxopropoxy)phenyl)cyclohexane (BMAPC) shows a potent microbial activity against bacterial and but moderately active against fungal species reported in our previous publication. This application attracted us to study its behavior in various solvents and also investigate its thermodynamic parameters. In the present work we have reported the measurements of density, viscosity, ultrasonic speed, and related acoustical and thermodynamic parameters of BMAPC solutions at different temperatures in order to study molecular interaction. The DO, EA, and THF were used as solvents for comparison of these properties due to its maximum solubility in these solvents as compared with other solvents. Lone pairs of electrons in three solvent systems which is more favorable for solute-solvent interactions. The structural formula of BMAPC is shown in Fig. 1.

EXPERIMENTAL

Ethyl acetate (EA), 1,4-dioxane (DO), and tetrahydrofuran (THF) used in the present investigation were supplied by Spectrochem Pvt. Ltd. Mumbai and were purified according to literature methods [12]. BMAPC used in this study was synthesized and crystallized in laboratory according to our previous publication [13].

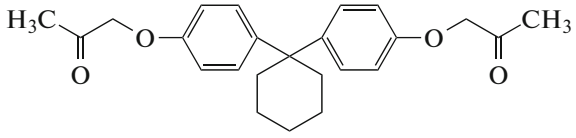

Fig. 1. 1,1-Bis(4-(2-oxopropoxy)phenyl)cyclohexane (BMAPC).

[1] The article is published in the original.

Table 1. The density (ρ), viscosity (η), and ultrasonic speed (U) data for BMAPC in DO, EA, and THF at 298, 303, 308, and 313 K

C, mol dm^{-3}	ρ, kg m^{-3}				η, mPa s				U, m s^{-1}			
	298 K	303 K	308 K	313 K	298 K	303 K	308 K	313 K	298 K	303 K	308 K	313 K
DO + BMAPC												
0.00	1027.6	1021.8	1016.2	1010.4	1.2224	1.0939	1.0100	0.9269	1344.9	1323.0	1301.1	1279.4
0.01	1028.1	1022.4	1016.8	1011.1	1.2234	1.0947	1.0108	0.9279	1346.1	1324.2	1302.4	1280.7
0.02	1028.7	1022.9	1017.5	1011.8	1.2260	1.0957	1.0124	0.9291	1347.3	1325.3	1303.6	1282.0
0.04	1029.8	1024.0	1018.5	1012.9	1.2275	1.0979	1.0139	0.9310	1349.7	1327.9	1306.1	1284.6
0.06	1030.8	1025.1	1019.7	1013.9	1.2299	1.1001	1.0161	0.9329	1351.9	1330.0	1308.2	1287.0
0.08	1031.9	1026.2	1020.8	1015.3	1.2328	1.1023	1.0182	0.9350	1354.3	1332.7	1311.1	1289.6
0.10	1032.9	1027.4	1021.9	1016.3	1.2356	1.1052	1.0210	0.9375	1356.7	1334.9	1313.4	1292.1
EA + BMAPC												
0.00	894.8	888.7	882.5	876.2	0.4274	0.4045	0.3844	0.3642	1140.5	1118.1	1095.6	1073.4
0.01	895.9	889.8	883.6	877.4	0.4284	0.4062	0.3854	0.3652	1142.4	1120.7	1097.7	1075.5
0.02	896.8	890.7	884.6	878.4	0.4293	0.4069	0.3864	0.3660	1144.2	1121.8	1099.4	1077.2
0.04	899.2	893.1	887.0	880.9	0.4312	0.4091	0.3885	0.3678	1147.5	1125.2	1102.9	1080.7
0.06	901.7	895.6	889.5	883.4	0.4335	0.4117	0.3910	0.3701	1151.4	1129.2	1107.0	1084.9
0.08	903.4	897.4	891.3	885.2	0.4347	0.4129	0.3922	0.3713	1154.0	1131.8	1109.6	1087.5
0.10	906.0	900.0	893.9	887.8	0.4371	0.4159	0.3948	0.3737	1158.1	1135.9	1113.8	1091.8
THF + BMAPC												
0.00	882.3	876.2	871.3	865.7	0.4632	0.4466	0.4305	0.4133	1278.3	1254.3	1230.3	1206.5
0.01	882.9	877.1	872.1	866.0	0.4636	0.4473	0.4310	0.4142	1278.8	1254.6	1230.7	1207.0
0.02	883.9	878.0	872.9	866.9	0.4644	0.4483	0.4322	0.4153	1279.8	1255.9	1232.0	1208.3
0.04	885.4	879.7	874.6	686.7	0.4660	0.4501	0.4342	0.4175	1282.0	1258.0	1234.2	1210.6
0.06	887.1	881.6	876.4	870.5	0.4678	0.4521	0.4363	0.4196	1283.9	1260.1	1236.4	1212.8
0.08	888.8	883.4	878.1	872.4	0.4693	0.4539	0.4383	0.4218	1285.8	1262.1	1238.4	1215.1
0.10	890.5	885.2	879.8	874.3	0.4711	0.4560	0.4404	0.4239	1287.9	1264.2	1240.6	1217.2

Measurements and Data Processing

A fresh stock solutions (0.1 M) of BMAPC in DO, EA, and THF were prepared. From the stock solutions, a series of dilute solutions (0.01 to 0.1 M) were prepared for a binary system and stored at room temperature for 24 h to ensure their solubility. Samples were kept in air-tight bottles until further use. The ρ, η, and U data of pure solvents are reported in Table 1 and were found comparable with literature values [14–17].

The ρ and U measurements were carried out on a Density and Sound Velocity Meter (DSA-5000 M) supplied by Anton Paar, Austria. Viscosity (η) measurements were carried out by using Ubbelohde type viscometer. The viscosity measurements were repeated at least three times for each sample. A constant temperature bath (Nova Instruments, Ahmedabad, Model NV8550E) with an accuracy of ±0.1 K was used for maintaining constant temperature during viscosity measurements. The flow times of pure solvents and solutions were measured with a digital RACER HS 10W stop watch with an accuracy of ±0.01 s. The solutions were prepared by mass using an analytical balance (AB 204-S; Mettler Toledo, Switzerland) with an uncertainty of $\pm 1 \times 10^{-4}$ kg.

Various acoustical and thermodynamic parameters were determined according to following theoretical equations mentioned in our recent publication [18, 19].

Acoustical parameters.

(1) Specific acoustical impedance:

$$Z = U\rho, \quad (1)$$

(2) adiabatic compressibility:

$$\kappa_a = \frac{1}{U^2\rho}, \quad (2)$$

(3) internal pressure:

$$\pi = b'RT\left(\frac{K'\eta}{U}\right)^{1/2}\frac{\rho^{2/3}}{M^{7/6}}, \quad (3)$$

where b' is the packing factor (2), K' is a constant (4.28×10^9), and R is the gas constant (8.314 J K^{-1} mol^{-1}),

(4) free volume:

$$V_f = \left[\frac{MU}{K'\eta}\right]^{3/2}, \quad (4)$$

(5) inter molecular free path length:

$$L_f = K_J(\kappa_a)^{1/2}, \quad (5)$$

where K_J is the Jacobson's constant ($K_J = (93.875 + 0.375T) \times 10^{-8}$) and it is temperature dependent,

(6) Van der Waals constant:

$$b = \frac{M}{\rho}\left[1 - \left[\frac{RT}{MU^2}\right]\left[\sqrt{1 + \frac{MU^2}{3RT}} - 1\right]\right], \quad (6)$$

where M is the apparent molecular weight of the solution, R is the gas constant, and T is the absolute temperature,

(7) viscous relaxation time (the resistance offered by viscous force in the flow of sound wave appears as a classical absorption associated with it is the viscous relaxation time):

$$\tau = \frac{4\eta}{3\rho U^2}, \quad (7)$$

(8) classical absorption coefficient:

$$(\alpha/f^2)_{cl} = \frac{8\pi^2\eta}{3U^3\rho}, \quad (8)$$

(9) Rao's molar sound function:

$$R_m = \frac{M}{\rho}U^{1/3}, \quad (9)$$

(10) solvation number:

$$S_n = \frac{M_2}{M_1\left(1 - \frac{\kappa_a}{\kappa_{a_1}}\right)\left(\frac{100 - X}{X}\right)}, \quad (10)$$

where M_1 and M_2 are the molecular weights of solvent and solute, respectively.

Thermodynamic Parameters

Free energy of activation (ΔG^*), enthalpy of activation (ΔH^*), and entropy of activation (ΔS^*) can be determined by using viscous relaxation time data at different concentrations and temperatures:

$$\frac{1}{\tau} = \frac{kT}{h}\exp\left(-\frac{\Delta G^*}{RT}\right), \quad (11)$$

$$\ln\frac{1}{\tau T} = \ln\frac{k}{h} + \frac{\Delta S^*}{R} - \frac{\Delta H^*}{RT}, \quad (12)$$

where k is the Boltzmann constant and h is the Planck's constant.

RESULTS AND DISCUSSION

Experimentally derived quantities such as, ρ, η, and U of pure solvents (DO, EA, and THF) and BMAPC solutions at four different temperatures: 298, 303, 308, and 313 K are presented in Table 1. The observed trend for ρ, η, and U is DO > EA > THF, DO > THF > EA, and DO > THF > EA. The ρ, η, and U data were correlated with C and T, and excellent correlation of these parameters with C and T is found (regression coefficient $R^2 = 0.9927–0.999$). The variations of η and U with C and T are considerably more than that of ρ due to specific solvent and solute interaction. The nature of solvents and solute play an important role, such as association, dissociation, H-bonding, etc. occurring in the solutions.

Various acoustical and thermodynamic parameters of pure solvents and solutions of BMAPC were derived according to Eqs. (1)–(12). Using ρ, η, and U data, various acoustical of BMAPC solutions were derived and correlated with C at different T. The variation of Z, κ_a, π, V_f, L_f, b, τ, $(\alpha/f^2)_{cl}$, and R_m with concentration at 30°C for all the solvent systems studied. The least-squares equations along with regression coefficients (R^2) are presented in Tables 2–4, from which it is observed that excellent correlation between a given parameter and concentration of BMAPC is found at different temperatures. U, Z, R_m, b, and V_f were increased linearly with C and decreased with T, while K_a, L_f, π, and τ and $(\alpha/f^2)_{cl}$ were decreased with C and increased with T. Either linear increase or decrease of specific acoustical parameters confirmed presence of strong molecular interactions in the solutions.

Variation of U in the solution depends upon intermolecular free path length. This can be attributed to the fact that the solvated molecules were fully compressed by the electrical forces of the solute. The strong solvent-solute interactions led to decrease of compressibility. Due to molecular association (solvent-solute interactions) compressibility of the solution decreased with the increasing solute concentration. Inter molecular free path length is inversely proportional to ultrasonic speed. It was observed from the results that L_f was decreased with C and increased with T further supported the presence of stronger molecular interactions. $(\alpha/f^2)_{cl}$ were decreased with C and increased with T. The presence of solvent–solute

Table 2. The least-square equations and regression coefficients (R^2) for BMAPC solutions in DO at 298, 303, 308, and 313 K

Parameter	298 K	303 K	308 K	313 K
ρ, kg m^{-3}	66.04C + 1027	67.08C + 1021	68.08C + 1016	69.15C + 1010
	(0.999)	(0.999)	(0.999)	(0.999)
η, mPa s	0.1293C + 1.2225	0.1119C + 1.0936	0.1073C + 1.0099	0.1035C + 0.9269
	(0.9921)	(0.9963)	(0.9953)	(0.9983)
U, m s^{-1}	95.35C + 1346	98.51C + 1324	100.8C + 1302	102.9C + 1280
	(0.999)	(0.999)	(0.999)	(0.999)
$Z \times 10^{-6}$, kg m^{-2} s^{-1}	0.1929C + 1.3821	0.1963C + 1.3518	0.1999C + 1.3223	0.2028C + 1.2929
	(0.9997)	(0.9998)	(0.9997)	(0.9998)
$\kappa_s \times 10^{10}$, Pa^{-1}	−1.2007C + 5.3796	−1.2981C + 5.5913	−1.4016C + 5.58122	−1.5186C + 6.0448
	(0.9997)	(0.9998)	(0.9995)	(0.9998)
$L_f \times 10^{11}$, m	−0.6506C + 5.1478	−0.6123C + 5.0478	−0.578C + 4.9509	−0.5449C + 4.8563
	(0.9998)	(0.9995)	(0.9998)	(0.9997)
$R_m \times 10^4$, m$^{10/3}$ s$^{-1/3}$ mol^{-1}	13.658C + 9.4638	13.716C + 9.4661	13.787C + 9.4648	13.874C + 9.4649
	(1)	(1)	(1)	(1)
$b \times 10^5$, m^3	11.737C + 8.0772	11.838C + 8.1135	11.942C + 8.1477	12.062C + 8.1835
	(1)	(1)	(1)	(1)
$\pi \times 10^{-8}$, Pa	−7.7272C + 5.3379	−7.5074C + 5.1559	−7.3966C + 5.0600	−7.2661C + 4.9492
	(0.9983)	(0.9981)	(0.9982)	(0.9982)
$V_f \times 10^7$, m^3	2.4248C + 1.077	2.8268C + 1.242	3.1237C + 1.3649	3.4823C + 1.5137
	(0.999)	(1)	(1)	(1)
$\tau \times 10^{13}$, s	−1.0502C + 8.7691	−1.0775C + 8.1529	−1.076C + 7.8265	−1.0634C + 7.4708
	(0.9949)	(0.9972)	(0.9961)	(0.9948)
$(\alpha/f^2)_{cl} \times 10^{15}$, s^2 m^{-1}	−2.6407C + 12.857	−2.6845C + 12.152	−2.7252C + 11.861	−2.7539C + 11.514
	(0.9982)	(0.9985)	(0.9979)	(0.9992)

interactions can also be confirmed from dispersion of ultrasonic speed, which is characterized by relaxation process. According to Eyring rate theory τ is inversely proportional to temperature and hence, increase in the temperature of system caused to decrease in relaxation process. τ is decreased with C and increased with T. R_m and b increased with C and T suggested absence of complex formation and practically independent of temperature. Decrease of π with C and increase with T suggested decrease of cohesive forces, which resulted in increase of free path length and free volume. The results of π further supplemented decrease of κ_a and L_f confirmed association of solvent molecules around solute molecules and strongly depend upon ρ, U, and T at constant pressure. Decrease of π with C and increase with T suggested decrease of cohesive forces, which resulted in increase of free path length and free volume.

When an ultrasonic wave are incident in the solution, the molecules get perturbed. Since the medium has some elasticity and hence perturbed molecules regain their equilibrium positions. When a solute is added to a solvent, its molecules attract certain solvent molecules toward them. The phenomenon is known as compression and as limiting compressibility. The aggregation of solvent molecules around solute molecules cause considerable change in structural arrangement and as consequence ρ, η, and U of the solutions are affected. Molecular interactions, such as solvent-solute interactions, quantum mechanical dispersive forces and dielectric force may cause high degree of contraction or expansion. The time lag between the excitation and de-excitation processes is as an acoustical relaxation process, which either results increase in speed with frequency or decrease in the $(\alpha/f^2)_{cl}$ with frequency. Increasing temperature has two effects namely structure formation (intermolecular association) and structure destructions. The structure forming tendency is primarily due to solute–solvent interactions, while destruction of structure formed is due to structure fluctuations. When thermal energy is greater than that of interaction energy, it causes destruction of the structure formed previously.

Table 3. The least-square equations and regression coefficients (R^2) for BMAPC solutions in EA at 298, 303, 308, and 313 K

Parameter	298 K	303 K	308 K	313 K
ρ, kg m^{-3}	66.04C + 1027 (0.999)	67.08C + 1021 (0.999)	68.08C + 1016 (0.999)	69.15C + 1010 (0.999)
η, mPa s	0.0956C + 0.4274 (0.997)	0.1093C + 0.4048 (0.9927)	0.1024C + 0.3844 (0.9957)	0.0931C + 0.3642 (0.996)
U, m s^{-1}	95.35C + 1346 (0.999)	98.51C + 1324 (0.999)	100.8C + 1302 (0.999)	102.9C + 1280 (0.999)
$Z \times 10^{-6}$, kg m^{-2} s^{-1}	0.2833C + 1.0206 (0.9986)	0.2817C + 0.9938 (0.998)	0.2843C + 0.967 (0.9984)	0.2842C + 0.9406 (0.9984)
$\kappa_s \times 10^{10}$, Pa^{-1}	−3.5687C + 8.5887 (0.9984)	−3.8156C + 8.9951 (0.9974)	−4.1662C + 9.4354 (0.9981)	−4.4961C + 9.9006 (0.9981)
$L_f \times 10^{11}$, m	−1.288C + 6.1362 (0.9985)	−1.3459C + 6.2797 (0.9975)	−1.4355C + 6.4316 (0.9982)	−1.5128C + 6.5882 (0.9982)
$R_m \times 10^4$, m$^{10/3}$ s$^{-1/3}$ mol^{-1}	16.37C + 10.29 (1)	16.474C + 10.293 (1)	16.595C + 10.295 (1)	16.709C + 10.298 (1)
$b \times 10^5$, m^3	14.617C + 9.2013 (0.999)	14.785C + 9.251 (0.999)	14.958C + 9.3015 (0.999)	15.135C + 9.3529 (0.999)
$\pi \times 10^{-8}$, Pa	−4.8807C + 3.123 (0.9976)	−4.8244C + 3.1063 (0.9977)	−4.8464C + 3.0942 (0.9976)	−4.8673C + 3.0775 (0.9975)
$V_f \times 10^7$, m^3	10.19C + 4.0637 (0.999)	10.395C + 4.2883 (0.999)	11.068C + 4.4931 (0.999)	11.865C + 4.724 (1)
$\tau \times 10^{13}$, s	−0.9833C + 4.8953 (0.9994)	−0.8024C + 4.8551 (0.9995)	−0.9025C + 4.837 (0.999)	−1.0095C + 4.8087 (0.9993)
$(\alpha/f^2)_{cl} \times 10^{15}$, s^2 m^{-1}	−2.9376C + 8.4623 (0.999)	−2.6988C + 8.5596 (0.9992)	−2.9927C + 8.7035 (0.9988)	−3.2851C + 8.8321 (0.9988)

The plots of S_n against C for BMAPC at different temperatures are presented in Figs. 2–4 from which it is observed that S_n increased nonlinearly with C and decreased with T indicating competing solvent-solute and solute–solute interactions in the solutions. In DO and THF systems observed solvation effect is almost same but in EA system it is considerably lower than later systems. The lone pairs of electrons of THF, DO,

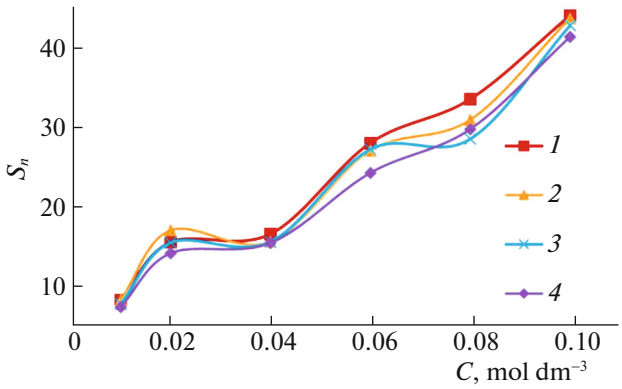

Fig. 2. The plots of solvation number (S_n) against concentration (C) for BMAPC in DO at 298 (*1*), 303 (*2*), 308 (*3*), and 313 K (*4*).

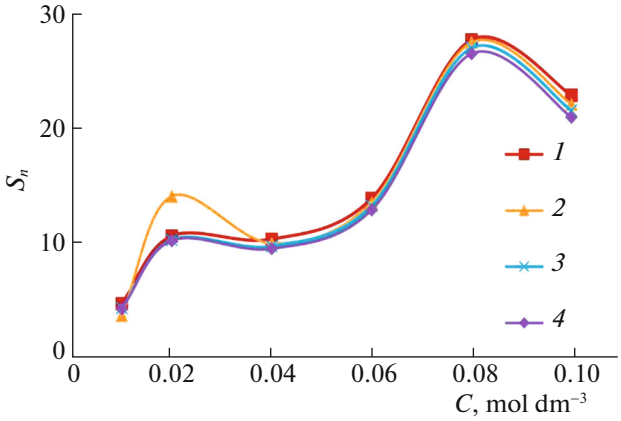

Fig. 3. The plots of solvation number (S_n) against concentration (C) for BMAPC in EA at 298 (*1*), 303 (*2*), 308 (*3*), and 313 K (*4*).

Table 4. The least-square equations and regression coefficients (R^2) for BMAPC solutions in THF at 298, 303, 308, and 313 K

Parameter	298 K	303 K	308 K	313 K
ρ, kg m^{-3}	66.04C + 1027	67.08C + 1021	68.08C + 1016	69.15C + 1010
	(0.999)	(0.999)	(0.999)	(0.999)
η, mPa s	0.0808C + 0.4629	0.0952C + 0.4464	0.1012C + 0.4302	0.1074C + 0.4132
	(0.9977)	(0.9991)	(0.9989)	(0.9998)
U, m s^{-1}	95.35C + 1346	98.51C + 1324	100.8C + 1302	102.9C + 1280
	(0.999)	(0.999)	(0.999)	(0.999)
$Z \times 10^{-6}$, kg m^{-2} s^{-1}	0.1931C + 1.1274	0.2031C + 1.0987	0.1977C + 1.0716	0.2071C + 1.0434
	(0.9988)	(0.9994)	(0.9993)	(0.9998)
$\kappa_s \times 10^{10}$, Pa^{-1}	−1.6888C + 6.9399	−1.8934C + 7.5583	−2.0123C + 7.5865	−2.2533C + 7.4952
	(0.9988)	(0.9991)	(0.9991)	(0.9995)
$L_f \times 10^{11}$, m	−0.6752C + 5.5158	−0.7405C + 5.6409	−0.7699C + 5.767	−0.8428C + 5.9018
	(0.9988)	(0.9991)	(0.9991)	(0.9995)
$R_m \times 10^4$, m$^{10/3}$ s$^{-1/3}$ mol^{-1}	18.662C + 8.8721	18.711C + 8.8766	18.888C + 8.8694	18.951C + 8.8754
	(1)	(1)	(1)	(1)
$b \times 10^5$, m^3	16.349C + 7.6436	16.469C + 7.6849	16.703C + 7.7168	16.838C + 7.7607
	(1)	(1)	(1)	(1)
$\pi \times 10^{-8}$, Pa	−7.6133C + 3.8345	−7.6085C + 3.8477	−7.6624C + 3.8622	−7.6634C + 3.8654
	(0.9962)	(0.9962)	(0.9962)	(0.9962)
$V_f \times 10^7$, m^3	10.335C + 3.1691	10.461C + 3.2527	10.706C + 3.3402	10.997C + 3.4469
	(1)	(1)	(1)	(1)
$\tau \times 10^{13}$, s	−0.3131C + 4.2835	−0.2297C + 4.3205	−0.1573C + 4.3521	−0.1358C + 4.3774
	(0.9982)	(0.9943)	(0.9986)	(0.9904)
$(\alpha/f^2)_{cl} \times 10^{15}$, s^2 m^{-1}	−0.983C + 6.6092	−0.9072C + 6.7943	−0.8471C + 6.9774	−0.8689C + 7.1563
	(0.9987)	(0.997)	(0.9986)	(0.9971)

ester group of EA and ether and ester groups of BMAPC are electronegative groups, while methyl and methylene hydrogens of EA are electropositive groups. The dipole–dipole interactions of opposite type resulted in the formation of H-bonding and of the same type resulted in the disruption of structure formed previously. Molecular association, resulted in the apparent structural change and hence density, viscosity, and ultrasonic speed change accordingly.

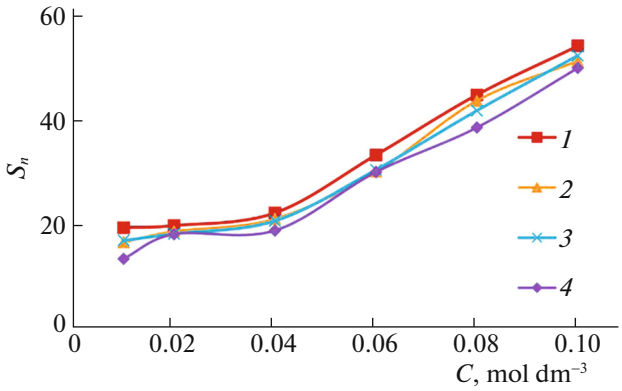

Fig. 4. The plots of solvation number (S_n) against concentration (C) for BMAPC in THF at 298 (*1*), 303 (*2*), 308 (*3*), and 313 K (*4*).

Thermodynamic parameters such as ΔG^*, ΔH^*, and ΔS^* were determined according to Eqs. (11) and (12) using viscous relaxation time data as a function of concentration and temperature are shown in Table 5. In DO system ΔG^* decreased with increasing C and T (R^2 = 0.9931–0.9981) while both ΔH^* and ΔS^* increased with increasing C. In EA system ΔG^* decreased with increasing C and T (R^2 = 0.9905–0.9993) and increased with increasing T, while both ΔH^* and ΔS^* increased slightly with C. In THF system ΔG^* decreased with increasing C (R^2 = 0.9957–0.9984) and increased with increasing T. Both ΔH^* and ΔS^* decreased with increasing C. Derived thermodynamic parameters indicated that condensation and evaporation processes are found concentration

Table 5. Thermodynamic parameters (ΔG^*, ΔH^*, and ΔS^*) derived using τ data for BMAPC in DO, EA, and THF solutions

System	ΔG^*, J mol^{-1}					ΔH^*, kJ mol^{-1}	ΔS^*, J K^{-1} mol^{-1}
	C	298 K	303 K	308 K	313 K		
DO + BMAPC	0.01	4196.0	4192.9	4130.1	4116.2	5.60	4.77
	0.02	4195.1	4189.5	4127.5	4112.5	5.61	4.80
	0.04	4186.7	4182.0	4118.8	4104.5	5.63	4.88
	0.06	4181.3	4176.0	4113.1	4097.1	5.65	4.85
	0.08	4175.5	4168.1	4104.4	4089.2	5.66	4.96
	0.1	4170.2	4163.2	4099.4	4083.4	5.67	4.98
EA + BMAPC	0.01	2749.6	2864.0	2896.3	2967.9	−1.65	−14.74
	0.02	2744.5	2859.2	2892.2	2962.3	−1.64	−14.71
	0.04	2743.33	2851.7	2881.1	2950.7	−1.61	−14.55
	0.06	2723.5	2842.6	2886.2	2939.7	−1.59	−14.47
	0.08	2714.9	2833.7	2862.9	2930.0	−1.60	−14.48
	0.1	2704.3	2825.9	2852.6	2918.1	−1.57	−14.35
THF + BMAPC	0.01	2422.2	2568.6	2629.6	2728.4	−3.69	−20.49
	0.02	2419.7	2567.0	2628.5	2727.3	−3.72	−20.59
	0.04	2416.0	2564.0	2626.9	2725.5	−3.76	−20.72
	0.06	2412.9	2560.9	2624.7	2723.8	−3.79	−20.82
	0.08	2408.9	2558.2	2622.8	2722.2	−3.85	−20.99
	0.1	2405.4	2556.1	2621.2	2720.6	−3.89	−21.11

and temperature dependent. The negative values of ΔH^* and ΔS^* indicated that activated complexes are highly in ordered state, i.e., condensation process is predominant over evaporation process, which is further supported by positive values of S_n with C. Thus, thermodynamic parameters supported presence of strong molecular interactions occurring in the solutions of different polarity.

CONCLUSIONS

Excellent correlation between studied acoustical and thermodynamic parameters with concentration and temperature was observed. Derived acoustical and thermodynamic parameters confirmed existence of strong molecular interactions in the solutions, which found to depend on molecular structure of the compound. ΔG^*, ΔH^*, and ΔS^* are observed to be dependent upon both concentration and temperature.

CONFLICTS OF INTEREST

The authors declare that they have no conflict of interest.

ACKNOWLEDGMENTS

The authors are thankful to UGC–New Delhi and DST–New Delhi for the instrumentation grants. Bhavin is also thankful to UGC–New Delhi for BSR Fellowship in Basic Science.

REFERENCES

1. R. K. Basal, J. Mittal, and P. Singh, J. Appl. Polym. Sci. **37**, 1901 (1989).
2. B. F. Sels et al., Green Chem. **16**, 1999 (2014).
3. H. K. Soni, V. S. Patel, and R. G. Patel, Thermochim. Acta **191**, 307 (1991).
4. N. A. Karmishina, E. N. Rodlovskaya, B. A. Izmailov, V. A. Vasnev, and M. I. Buzin, Russ. J. Appl. Chem. **85**, 674 (2012).
5. K. Sumoto, N. Mibu, K. Yokomizo, and M. Uyeda, Chem. Pharm. Bull. **52**, 298 (2002).
6. R. Amorati, M. Lucarini, V. Mugnaini, and G. F. Pedulli, J. Org. Chem. **68**, 5198 (2003).
7. A. Dhote and S. Aswale, Adv. Appl. Sci. Res. **3**, 2299 (2012).
8. V. Frenkle, Adv. Drug. Deliv. Rev. **60**, 1193 (2008).
9. D. R. Godhani, P. B. Dobariya, A. M. Sanghani, A. A. Jogel, and J. P. Mehta, J. Mol. Liq. **180**, 179 (2013).

10. G. M. Kumar and S. A. Kumar, Russ. J. Chem. Sci. **3**, 27 (2012).
11. B. R. Shinde and K. M. Jadhav, J. Eng. Res. Stud. **1**, 128 (2010).
12. A. I. Vogel, A. R. Tatchell, B. S. Furnis, A. J. Hannaford, and P. W. D. Smith, *Vogel's Textbook of Practical Organic Chemistry,* 5th ed. (Addison Wesley Longman, London, 1998).
13. B. B. Dhaduk, C. B. Patel, and P. H. Parsania, Lett. Drug. Des. Discov. **12**, 152 (2015).
14. M. Habibullah, I. M. Rahman, M. A. Uddin, M. Anowar, M. Alam, K. Iwakabe, and H. Hasegawa, J. Chem. Eng. Data **58**, 2887 (2013).
15. M. Gupta, I. Vibhu, and J. Shukla, Fluid Phase Equilib. **244**, 26 (2006).
16. M. Gowrisankar, P. Venkateshwarlu, K. Sivakumar, and S. Sivarambabu, J. Solut. Chem. **42**, 916 (2013).
17. H. Djojoputro and S. Ismadji, J. Chem. Eng. Data **50**, 727 (2005).
18. B. B. Dhaduk, C. B. Patel, and P. H. Parsania, J. Solut. Chem. **44**, 1976 (2015).
19. B. B. Dhaduk, C. B. Patel, and P. H. Parsania, Russ. J. Phys. Chem. A **91**, 2495 (2017).